Available online at www.sciencedirect.com
SCIENCE DIRECT
International Journal of Mass Spectrometry 249–250 (2006) 206–214
International Journal of Mass Spectrometry
www.elsevier.com/locate/ijms

# Generation and characterization of ionic and neutral chloro(hydroxy) phosphanyl $[Cl–P–OH]^{+/\bullet}$ and chloro(thiohydroxy) phosphanyl $[Cl–P–SH]^{+/\bullet}$ in the gas phase by tandem mass spectrometry and computational chemistry☆

R. Srikanth [a], P. Nagi Reddy [a], K. Bhanuprakash [b], R. Srinivas [a,*]

[a] *National Center for Mass Spectrometry, Indian Institute of Chemical Technology, Hyderabad 500 007, India*
[b] *Inorganic Chemistry Division, Indian Institute of Chemical Technology, Hyderabad 500 007, India*

Received 14 September 2005; received in revised form 20 December 2005; accepted 20 December 2005
Available online 20 January 2006

This paper is dedicated to the memory of Chava Lifshitz, an eminent mass spectrometrist.

**Abstract**

Dissociative electron ionization (70 eV) of diethyl chlorothiophosphate (**I**) and ethylphosphonodichloridate (**II**) generates moderately abundant *m*/*z* 83 ions of composition [P, Cl, O, H]$^+$. From tandem mass spectrometry experiments and theoretical calculations at the B3LYP/6-31G(d, p), G2, and G2(MP2) levels it is concluded that the majority of the ions have the structure of $ClPOH^+$ (**1a**$^+$) and it is separated by high-energy barriers from its isomers $HP(O)Cl^+$ (**1b**$^+$), $HPOCl^+$ (**1c**$^+$), and OP–ClH (**1d**$^+$). Neutralization–reionization experiments confirm the theoretical prediction that radical **1a**$^\bullet$ is a stable species in the gas phase. The 70 eV electron ionization of ethylphosphonothioic dichloride (**III**) yields *m*/*z* 99 ions, predominantly of the structure $ClPSH^+$ (**2a**$^+$). This conclusion follows from tandem mass spectrometry experiments and theoretical calculations. The calculations predict that (**2a**$^+$) is separated by high-energy barriers from its isomers $HP(S)Cl^+$ (**2b**$^+$), $HPSCl^+$ (**2c**$^+$), and SP–ClH (**2d**$^+$). Neutralization–reionization experiments confirmed that **2a**$^\bullet$ radical is a stable species in the rarefied gas phase, which is in agreement with theoretical calculations.


*Keywords:* Chloro(hydroxy) phosphanyl; Chloro(thiohydroxy) phosphanyl; Collision induced dissociation; Neutralization–reionization; Computational chemistry

## 1. Introduction

Over the past 15 years, a great deal of attention has been focused on the chemistry of phosphorus oxoacids, some of which belong to the family of low coordinated phosphorus compounds. Phosphorus oxoacids are believed to play an important role in the chemistry and biochemistry of phosphorus and have been extensively studied by experiment and theory [1–5]. Low coordination dithiophosphanes are also known to be reactive intermediates and some of them have been isolated as stable ligands in complexes [6,7]. Unfortunately, direct evidence for the existence of these species as stable monomeric entities is scarce due to facile intermolecular reactions. The neutralization–reionization mass spectrometry (NRMS) technique [8–14] has been established as a powerful tool for investigating the stabilities and structures of highly reactive and elusive transient species in the rarefied gas phase and it has been successfully used to generate and characterize some of the low coordinated phosphorus species. Keck, Terlouw and their co-workers have provided NRMS experimental evidence for the gas phase existence of (methylthio) thioxophosphane ($CH_3S–P–S$) [15], phosphenethiol ($H_2P–SH$) [16], phosphenedithiol $HP(SH)_2$ [17], thioxophosphane HPS and its tautomer HSP [18] and phosphorotrithious acid $P(SH)_3$ [19] molecules. Gu and Tureček [20] have reported an NRMS study on several oxygenated phosphorus radicals, e.g., PO, $CH_3OPH$, $CH_3OPOH$, $CH_3OPOCH_3$, and $(CH_3O)_2PO$. Other low coordinated phosphorus species that have been studied includes $CH_3O–P=O$, $CH_3S–P=O$ [21], $NH_3PO$ [22], and $CH_3O–P–NH_2$ [23] by using a combination of tandem mass

☆ IICT Communication No. 050914.
* Corresponding author. Tel.: +91 40 27160123; fax: +91 40 27160387.
*E-mail address:* sragampeta@yahoo.co.in (R. Srinivas).

1387-3806/$ – see front matter © 2006 Elsevier B.V. All rights reserved.
doi:10.1016/j.ijms.2005.12.031

spectrometric techniques. Turecek et al. also have demonstrated the importance of Franck–Condon effects in the dissociations and isomerizations of gas phase phosphorus oxoacids and radicals, mainly $P(OH)_3$ and $P(OH)_4^{\bullet}$ and their corresponding isomeric species [24]. A number of theoretical calculations were also reported on these tri and tetra coordinated hydroxy and thiohydroxy phosphoranyl species [25–32]. We recently reported on the characterization of ionic and neutral $P(OH)_2^{+/\bullet}$, $HSPOH^{+/\bullet}$, $S{=}P(OH)_2^{+/\bullet}$ and the corresponding isomeric species by NRMS and computational chemistry [33,34]. In continuation of our studies, we report here on the generation and characterization of both ionic and neutral $[Cl–P–OH]^{+/\bullet}$ and $[Cl–P–SH]^{+/\bullet}$ by using a combination of tandem mass spectrometric experiments and theoretical calculations.

## 2. Experimental and theoretical methods

The mass spectrometric experiments reported here were carried out using a VG Micromass Autospec M mass spectrometer of $E_1BE_2$ geometry [21] (E denotes an electric sector and B, magnetic sector). The instrument has two collision chambers (Cls-2 and Cls-3) and an intermediate deflector electrode, all in the third field free region (between $E_1B$ and $E_2$).

Diethyl chlorothiophosphate (**I**) was commercially available (Aldrich) and used without further purification. Ethylphosphonodichloridate (**II**) and ethylphosphonothioic dichloride (**III**) used in the present study were synthesized in-house by reported methods [35,36]. The synthesized compounds were characterized by infrared, $^1H$ nuclear magnetic resonance, and mass spectral data. All the compounds were introduced into the ion source through the liquid inlet system under the following conditions: source temperature, 200 °C; electron energy, 70 eV; trap current 200 μA; acceleration potential, 7 kV. Accurate mass measurements of the ions at *m/z* 83 from **I** and **II** and *m/z* 99 from **III** were obtained at a resolution of $m/\Delta m = 5000$ (10% valley definition), using the data system. The collision induced dissociation (CID) mass spectra were recorded by mass selecting the beam of interest ions using $E_1B$ (MS-1), with 7 keV translational energy and allowing collisions with oxygen in the collision cell Cls-3, the resulting ions were analyzed by scanning $E_2$ (MS-2). CID mass spectra were also recorded in the FFR-1 using the linked scan technique (B/E = constant). The NR experiments were conducted by mass selecting the beam of precursor ions with $E_1B$ (MS-1) and neutralizing them in Cls-2 with xenon. The remaining ions were deflected away from the beam of neutrals by means of a deflector electrode (+5 kV). The neutral beam was reionized in Cls-3 with $O_2$ target gas and the resulting ions were recorded by scanning $E_2$. The spectra shown are accumulations of 25–50 scans.

Standard ab initio and density functional methods included in the Gaussian 03 [37] suites of programs were used to calculate the geometries and relative stabilities of ions and their corresponding neutral isomers. In the density functional methods, Becke's hybrid functional, B3LYP with the 6-31G(d, p) basis set was used initially for geometry optimizations [38], while in the ab initio methods G2 [39] and G2(MP2) [40] schemes were used. Stationary points were characterized as either minima (all real frequencies) or transition states (one imaginary frequency) by calculation of the frequencies using an analytical gradient procedure. The minima connected by given transition structures were confirmed by intrinsic reaction coordinate (IRC) calculations. The calculated frequencies were also used to determine zero-point vibrational energies, which were used as a zero-point correction for the electronic energies. Spin unrestricted calculations were used for all open shell systems and the spin contamination was not found to be high (0.75–0.76) for doublets.

## 3. Results and discussion

### 3.1. Preparation and dissociation of [P, Cl, O, H]$^+$ ions

The 70 eV electron-ionization mass spectra of diethyl chlorothiophosphate (**I**) and ethylphosphonodichloridate (**II**) afford a moderately abundant peak at *m/z* 83 (18% and 32% of the base peak, respectively) corresponding to $[P, Cl, O, H]^+$ ions. The elemental composition of this ion has been confirmed by high-resolution measurements and isobaric impurities were not detected. The formation of these ions from the diethyl chlorothiophosphate ($\mathbf{I}^{\bullet+}$) can be envisaged to proceed by two different pathways: (1) $188^{\bullet+}(\mathbf{I}^{\bullet+}) \rightarrow 144^{\bullet+} \rightarrow 116^{\bullet+} \rightarrow 83^+$, i.e., loss of acetaldehyde molecule followed by successive losses of ethylene and $SH^{\bullet}$ radical, (2) $188^{\bullet+}(\mathbf{I}^{\bullet+}) \rightarrow 144^{\bullet+} \rightarrow 111^+ \rightarrow 83^+$, i.e., loss of acetaldehyde molecule followed by $SH^{\bullet}$ radical and ethylene molecule. For $\mathbf{II}^{\bullet+}$, the *m/z* 83 ions are generated by two routes: (1) $146^{\bullet+}(\mathbf{II}^{\bullet+}) \rightarrow 111^+ \rightarrow 83^+$, i.e., loss of chlorine radical followed by ethylene molecule, (2) $146^{\bullet+}(\mathbf{II}^{\bullet+}) \rightarrow 118^+ \rightarrow 83^+$, i.e., loss of ethylene molecule followed by chlorine radical (Scheme 1). Evidence for these pathways follows from metastable ion (MI) spectra of the molecular ions and the intermediate ions.

The *m/z* 83 ions were characterized by MI and CID spectra; the latter were recorded as B/E and MIKE scans. The metastable ion spectrum shows $PCl^+$ (*m/z* 66), $PO^+$ (*m/z* 47) and $POH^{\bullet+}$ (*m/z* 48) ions corresponding to losses of $OH^{\bullet}$, HCl and $Cl^{\bullet}$, respectively.

The CID spectra (B/E and MIKE) of *m/z* 83 ions display the base peak at *m/z* 48 ($POH^{\bullet+}$) due to loss of $Cl^{\bullet}$ and other abundant fragment ions at *m/z* 66 (loss of $OH^{\bullet}$), *m/z* 47 (loss of HCl) and *m/z* 82 (loss of $H^{\bullet}$) corresponding with the fragment ions $[PCl]^+$, $[PO]^+$ and $[ClPO]^{\bullet+}$, respectively. Moderately abundant peaks are observed at *m/z* 35 $[Cl]^+$ and at *m/z* 31 $[P^+]$. The CID spectra of the *m/z* 83 ions from ethylphosphonodichloridate (**II**) are found to be identical with those from diethyl chlorothiophosphate (**I**). The representative MIKE CID spectrum is presented in Fig. 1a. With all these structure indicative peaks, the spectra are most compatible with the Cl–P–$OH^+$ ($\mathbf{1a}^+$) bond connectivity for the *m/z* 83 ions. This proposal is further supported by the CID spectrum of *m/z* 85 ions corresponding with the $[P, {}^{37}Cl, O, H]^+$ ions (Fig. 2a). It should be noted that the spectrum displays peaks at *m/z* 84, *m/z* 68, and *m/z* 37 corresponding with $^{37}ClPO^{\bullet+}$, $^{37}ClP^{\bullet+}$, and $^{37}Cl^+$ ions. Both the spectra (Figs. 1a and 2a) show low abundance artifact signals which may possibly arise due to minor contributions

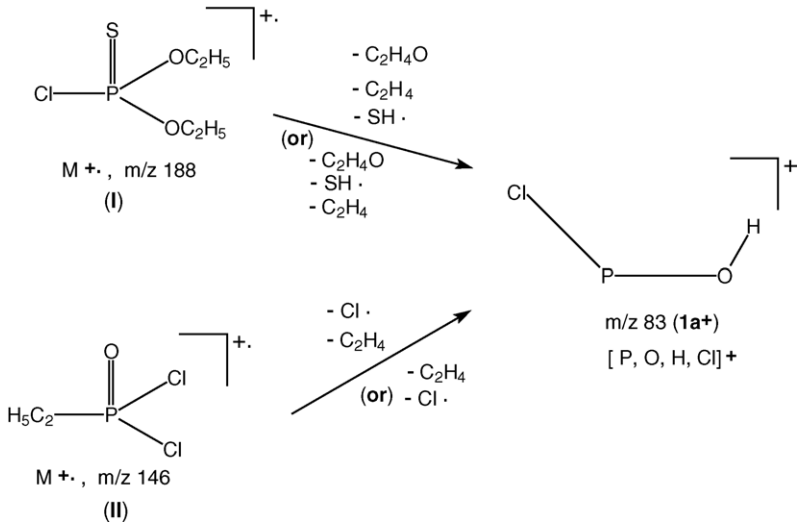


Scheme 1.

from decompositions occurring in the second FFR. For e.g., decompositions of *m*/*z* 116/118 ions in to *m*/*z* 98/100.

### 3.2. Ion structures and energetics

To interpret the experimental data from ion dissociations, we investigated by calculations the potential energy surface for dissociations and isomerizations of all possible isomers $\mathbf{1a}^+$–$\mathbf{1d}^+$ (Table 1). The results from B3LYP/6-31G(d, p) calculations are summarized diagrammatically in Scheme 2, the optimized ion structures and transition state geometries are shown in Fig. 3. Ion $\mathbf{1a}^+$ is the most stable structure of the four studied. It has a $C_S$ symmetry with syn arrangement of the O–H and Cl bonds that corresponds to the lowest-energy orientation of the correspond-

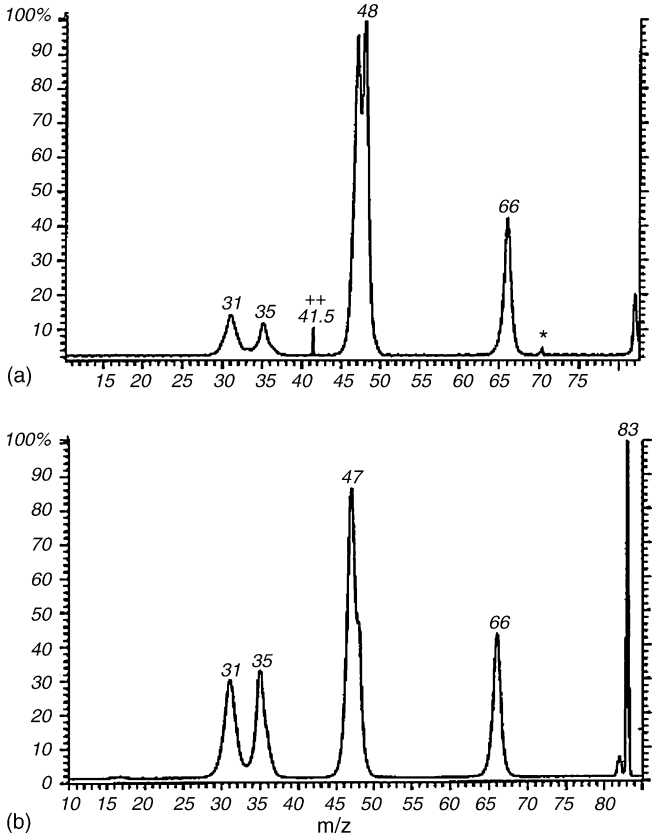


Fig. 1. (a) MIKES CID spectrum ($O_2$, 70% T) and (b) NR spectrum (Xe, 70% T/$O_2$, 70% T) of *m*/*z* 83 [P, $^{35}$Cl, O, H]$^+$ ions from diethyl chlorothiophosphate (**I**).

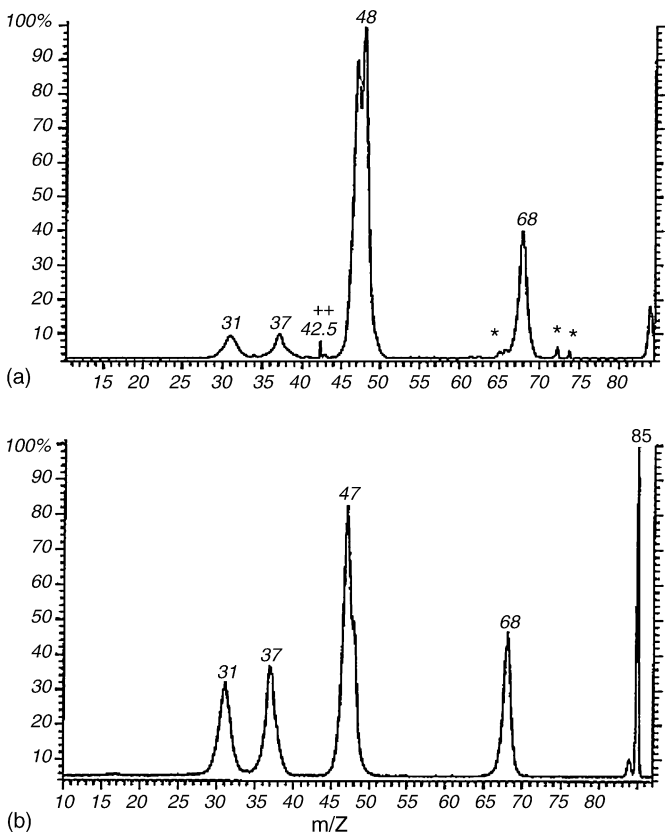


Fig. 2. (a) MIKES CID spectrum ($O_2$, 70% T) and (b) NR spectrum (Xe, 70% T/$O_2$, 70% T) of *m*/*z* 85 [P, $^{37}$Cl, O, H]$^+$ ions from diethyl chlorothiophosphate (**I**).

Table 1
Total (a.u.) and relative energies (kcal mol$^{-1}$) of [P, O, H, Cl] ions calculated using various methods

| Species | G2 (0 K) | G2(MP2) (0 K) | B3LYP/6-31G(d, p)[a] |
|---|---|---|---|
| ClPOH$^+$ (**1a**$^+$) ($C_S$) | −876.111143 (0.0) | −876.099143 (0.0) | −877.065392 (0.0) |
| HP(O)Cl$^+$ (**1b**$^+$) ($C_S$) | −876.066354 (28.1) | −876.053998 (28.3) | −877.013441 (32.6) |
| HPOCl$^+$ (**1c**$^+$) ($C_S$) | −875.979482 (82.6) | −875.966305 (83.3) | −876.942994 (76.8) |
| OP–ClH (**1d**$^+$) ($C_S$) | −876.078591 (20.4) | −876.067353 (19.9) | −877.039371 (16.3) |
| TS **1a**$^+$–**1b**$^+$ ($C_1$) | −875.998045 (70.9) | −875.987386 (70.1) | −876.947425 (74.0) |
| TS **1b**$^+$–**1c**$^+$ ($C_1$) | −875.939417 (107.7) | −875.926969 (108.0) | −876.894808 (107.0) |
| TS **1a**$^+$–**1d**$^+$ ($C_1$) | −876.043944 (42.2) | −876.032878 (41.6) | −876.998368 (42.1) |
| TS **1b**$^+$–**1d**$^+$ ($C_1$) | −875.987969 (77.3) | −875.977394 (76.4) | −876.937991 (79.9) |
| POH$^{\bullet+}$ + Cl$^\bullet$ *m/z* 48 | −875.963199 (92.8) | −875.948753 (94.4) | −876.936412 (80.9) |
| PO$^+$ + HCl *m/z* 47 | −876.056665 (34.2) | −876.04579 (33.5) | −877.019001 (29.1) |
| PCl$^{\bullet+}$ + OH$^\bullet$ *m/z* 66 | −875.920176 (119.8) | −875.907422 (120.3) | −876.885633 (112.8) |
| ClPO$^{\bullet+}$ + H$^\bullet$ *m/z* 83 | −875.918545 (120.8) | −875.906148 (121.1) | −876.887424 (111.7) |

[a] ZPE corrected.

ing bond dipoles. Ions **1b**$^+$ and **1c**$^+$ are 32.6 and 76.8 kcal mol$^{-1}$ less stable than **1a**$^+$ respectively. Ions **1a**$^+$ and **1b**$^+$ are separated by an energy barrier (41.4 kcal mol$^{-1}$ above **1b**$^+$). Similarly, **1b**$^+$ and **1c**$^+$ ions are separated by an energy barrier (30.3 kcal mol$^{-1}$ above **1c**$^+$). Thus it is likely that most of the *m/z* 83 ions will have Cl–P–OH$^+$ (**1a**$^+$) structure and significant contribution of **1b**$^+$–**1c**$^+$ can be ruled out. Further support for this proposal follows from the absence of a peak at *m/z* 32 (HP$^{\bullet+}$) in the CID spectrum (Fig. 1a), which is expected for isomers **1b**$^+$ and **1c**$^+$.

The isomer **1d**$^+$ (dimer of PO and ClH) is second most stable isomer, 16.3 kcal mol$^{-1}$ less stable than **1a**$^+$. Ions **1a**$^+$ and **1d**$^+$ are separated by an energy barrier (25.8 kcal mol$^{-1}$ above **1d**$^+$), which is above the dissociation energy for the formation of PO$^+$ + HCl (29.1 kcal mol$^{-1}$). This implies that loss of HCl involves isomerization of **1a**$^+$ to **1d**$^+$ prior to dissociation. **1d**$^+$ is also separated from **1b**$^+$ by an energy barrier (47.3 kcal mol$^{-1}$ above **1b**$^+$). Thus based on all these results, it can be proposed that the CID spectra of *m/z* 83 ions represent a mixture of **1a**$^+$/**1d**$^+$ ions. However, for energetic and entropic reasons most of the ions are expected to have the connectivity **1a**$^+$.

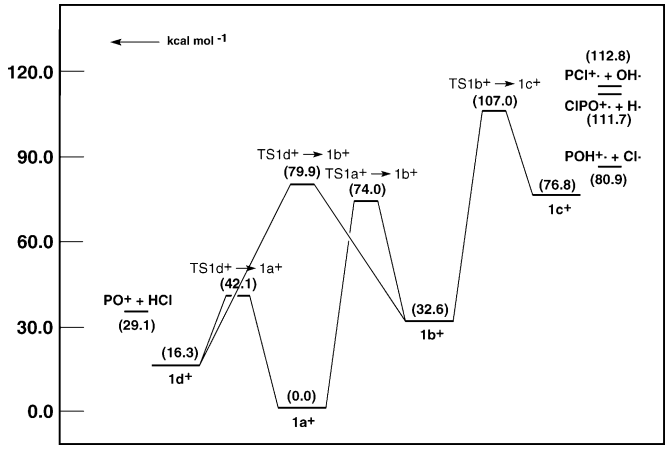


Scheme 2. Potential energy diagram from B3LYP/6-31G(d, p) calculations for the rearrangement and dissociation reactions of ions **1a**$^+$–**1d**$^+$.

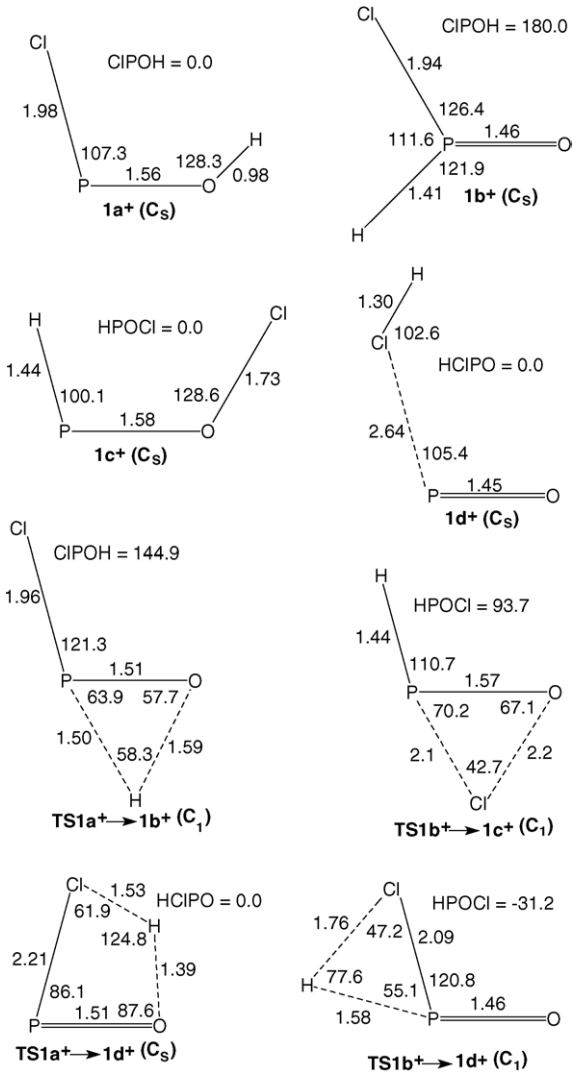


Fig. 3. Selected optimized geometries of ionic [P, Cl, O, H]$^+$ isomers **1a**$^+$–**1d**$^+$, connecting transition states from B3LYP/6-31G(d, p) calculations.

### 3.3. Preparation and dissociation of [P, Cl, O, H]• radicals

The neutralization (Xe, 70%)–reionization ($O_2$, 70%) mass spectrum of *m/z* 83 ions shows recovery signal as the base peak (Fig. 1b). The spectrum shows all the fragment ions that are seen in the CID spectrum of Fig. 1a, except that the relative abundances of *m/z* 48, *m/z* 82 are decreased and those of *m/z* 47, *m/z* 35, *m/z* 31 are increased in the NR spectrum. Weakly abundance peaks at *m/z* 16–18 are also present in the spectrum. The presence of a high abundance recovery signal, indicates that vertical neutralization of $\mathbf{1a}^+$ ions yield neutral species that are stable on the NR experimental time-scale of microseconds and have retained the $\mathbf{1a}^\bullet$ connectivity. The doubly charged ions are absent in the NR spectrum which can be attributed to a lower probability for the $M \rightarrow M^{2+}$ compare to the $M^{\bullet+} \rightarrow M^{2+}$ process [41].

This proposal is further supported by the NR spectrum of *m/z* 85 ions (Fig. 2b) corresponding with the composition [P, $^{37}$Cl, O, H]$^+$ ions. The spectrum is identical with that of *m/z* 83 ions (Fig. 1b), in the way that now the spectrum exhibits all $^{37}Cl^+$ containing ions instead of $^{35}Cl^+$ ions viz., *m/z* 84 $[^{37}ClPO]^{\bullet+}$, *m/z* 68 $[^{37}ClP]^+$ and *m/z* 37 $[^{37}Cl]^+$ ions.

### 3.4. Radical structures and energetics

These experimental results are consistent with the theoretical calculations (Table 2 and Fig. 4), which show $\mathbf{1a}^\bullet$ as the global minimum and stable with respect to dissociation. In contrast to the cation relative stabilities, $\mathbf{1b}^\bullet$ is second most stable isomer and 11.6 kcal mol$^{-1}$ less stable than $\mathbf{1a}^\bullet$. $\mathbf{1a}^\bullet$ and $\mathbf{1b}^\bullet$ are separated by substantial energy barrier of 43.2 kcal mol$^{-1}$. $\mathbf{1c}^\bullet$ is 65.4 kcal mol$^{-1}$ less stable than $\mathbf{1a}^\bullet$. In contrast to the structure of $\mathbf{1d}^+$, $\mathbf{1d}^\bullet$ has optimized to a different structure which is 22.2 kcal mol$^{-1}$ less stable than $\mathbf{1a}^\bullet$, and separated by an energy barrier of 37.9 kcal mol$^{-1}$.

Further support for the stability of the transient neutral comes from an examination of the Franck–Condon effects on vertical electron capture by the corresponding cations. For $\mathbf{1a}^+$, the calculated vertical ionization energy of the neutral ($IE_V$) is found to be 12.2 kcal mol$^{-1}$ (Table 3) higher than the adiabatic process, and vertical neutralization ($RE_V$) of thermalized Cl–P–OH$^+$ ions differ by only 7.2 kcal mol$^{-1}$ from the adiabatic process. The minimum excess Franck–Condon energy of Cl–P–OH$^\bullet$ is only 7.2 kcal mol$^{-1}$, which is insufficient to induce any dissociation or isomerization as the threshold energy of dissociation or isomerization lies at higher energies (Table 3). Thus the observed recovery signal in the NR spectrum should correspond to the $\mathbf{1a}^\bullet$ survivor ions.

In contrast, vertical neutralization of $\mathbf{1d}^+$ leads to $\mathbf{1d}^\bullet$ with a different structure which probably dissociate into PO$^\bullet$ + HCl.

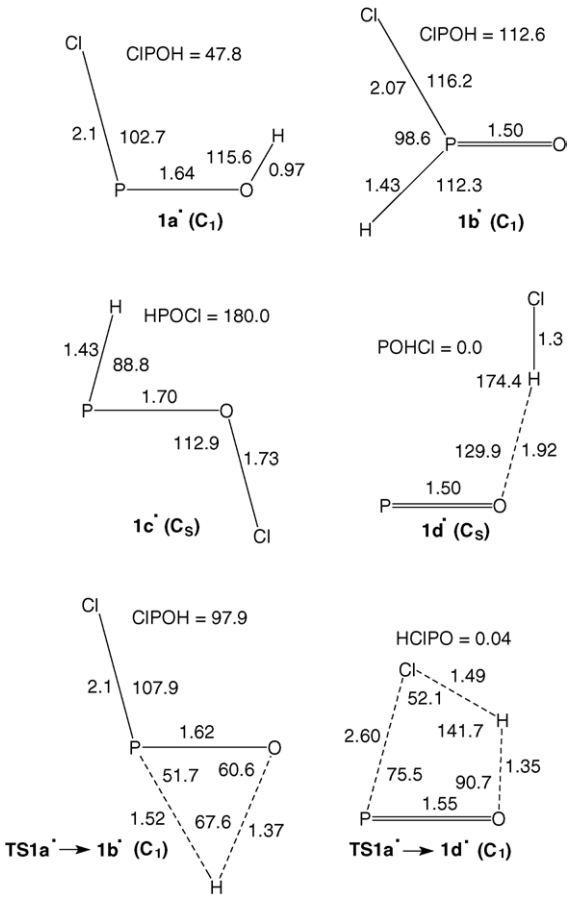


Fig. 4. Selected optimized geometries of neutral [P, Cl, O, H]• isomers $\mathbf{1a}^\bullet$–$\mathbf{1d}^\bullet$ and connecting transition states from B3LYP/6-31G(d, p) level.

Table 2
Total (a.u.) and relative energies (kcal mol$^{-1}$) of [P, O, H, Cl] radicals calculated using various methods

| Species | G2 (0 K) | G2(MP2) (0 K) | B3LYP/6-31G(d, p)[a] |
|---|---|---|---|
| ClPSH• (**1a**•) ($C_1$) | −876.399936 (0.0) | −876.385355 (0.0) | −877.363965 (0.0) |
| HP(S)Cl• (**1b**•) ($C_1$) | −876.386895 (8.2) | −876.373131 (7.7) | −877.345427 (11.6) |
| HPSCl• (**1c**•) ($C_1$) | −876.291697 (67.9) | −876.276241 (68.5) | −877.259662 (65.4) |
| PO–HCl• (**1d**•) ($C_S$) | −876.370324 (18.6) | −876.355634 (18.6) | −877.328530 (22.2) |
| TS **1a**•–**1b**• ($C_1$) | −876.330257 (43.7) | −876.315674 (43.7) | −877.2950641 (43.2) |
| TS **1a**•–**1d**• ($C_1$) | −876.336199 (39.9) | −876.322150 (39.7) | −877.303602 (37.9)) |
| ClPO + H• *m/z* 82 | −876.337797 (38.9) | −876.324309 (38.3) | −877.291804 (45.3) |
| POH + Cl• *m/z* 48 | −876.249585 (94.3) | −876.232069 (96.2) | −877.215878 (92.9) |
| Cl• + POH *m/z* 35 | −876.249585 (94.3) | −876.232069 (96.2) | −877.215878 (92.9) |
| PO• + HCl *m/z* 47 | −876.364478 (22.2) | −876.349381 (22.6) | −877.321820 (26.6) |
| PCl + OH• *m/z* 66 | −876.221164 (112.2) | −876.205213 (113.0) | −877.183719 (113.1) |

[a] ZPE corrected.

Table 3
Calculated adiabatic energies ($IE_a$) and vertical one-electron transition energies (in eV) of ions and neutrals of $[P, O, H, Cl]^{+/\bullet}$ isomers at B3LYP/6-31G(d, p)

| Transitions | $IE_a$[a] | $RE_v$ | $IE_v$ |
|---|---|---|---|
| **1a**$^+ \rightarrow$ **1a**$^\bullet$ | 8.09 | 7.78 | |
| **1a**$^\bullet \rightarrow$ **1a**$^+$ | | | 8.62 |
| **1b**$^+ \rightarrow$ **1b**$^\bullet$ | 9.00 | 7.74 | |
| **1b**$^\bullet \rightarrow$ **1b**$^+$ | | | 10.09 |
| **1c**$^+ \rightarrow$ **1c**$^\bullet$ | 8.59 | 8.39 | |
| **1c**$^\bullet \rightarrow$ **1c**$^+$ | | | 8.80 |

$RE_v$ and $IE_v$ represents recombination (neutralization) and ionization energies, respectively.
[a] Without ZPE corrections.

Also neutralization of **1b**$^+$ and **1c**$^+$ can lead to **1b**$^\bullet$ and **1c**$^\bullet$ with internal energies (Table 3) that are sufficient to induce fragmentation. These neutral species, PO$^\bullet$ and other dissociation products P$^\bullet$, Cl$^\bullet$, on re-ionization can contribute to the enhancement of the signals at *m/z* 47, *m/z* 31 and *m/z* 35 in the NR spectrum. Thus these effects may account for the enhanced peaks in the NR spectrum as well as the high abundance survivor signal for ClPOH$^\bullet$ (**1a**$^\bullet$).

### 3.5. Preparation and dissociation of $[P, Cl, S, H]^+$ ions

The 70 eV electron-ionization mass spectra of ethylphosphonothioic dichloride (**III**) afford a moderately abundant peak at *m/z* 99 (20% of the base peak) corresponding to $[P, Cl, S, H]^+$ ions. The elemental composition of this ion has been confirmed by high-resolution measurements and isobaric impurities were not detected. The formation of these ions from the ethylphosphonothioic dichloride (**III**) can be envisaged to proceed by two different pathways: (1) $162^{\bullet+}$(**III**$^{\bullet+}$) $\rightarrow 127^+ \rightarrow 99^+$, i.e., loss of chlorine radical followed by ethylene molecule, (2) $162^{\bullet+}$(**III**$^{\bullet+}$) $\rightarrow 134^{\bullet+} \rightarrow 99^+$, i.e., loss of ethylene molecule followed by Cl$^\bullet$ radical (Scheme 3). Evidence for these pathways follows from metastable ion (MI) spectra of the molecular ions and the intermediate ions.

The *m/z* 99 ions were also characterized by MI and CID spectra. The MI spectrum shows $PCl^+$ (*m/z* 66), $PS^+$ (*m/z* 63) and $PSH^{\bullet+}$ (*m/z* 64) ions corresponding to losses of SH$^\bullet$, HCl and Cl$^\bullet$, respectively. The CID spectra (B/E and MIKE) display the base peak at *m/z* 63 $[PS]^+$ due to loss of HCl and other abundant fragment ions are $[PCl]^+$ at *m/z* 66, $[PSH]^{\bullet+}$ at *m/z* 64 (loss of Cl$^\bullet$), and $[ClPS]^{\bullet+}$ at *m/z* 98 (loss of H$^\bullet$). Low abundant peaks are observed at *m/z* 35 $[Cl]^+$, at *m/z* 31 $[P^+]$ and at *m/z* 32 $[S]^{\bullet+}$. The representative MIKE CID spectrum is presented in Fig. 5a.

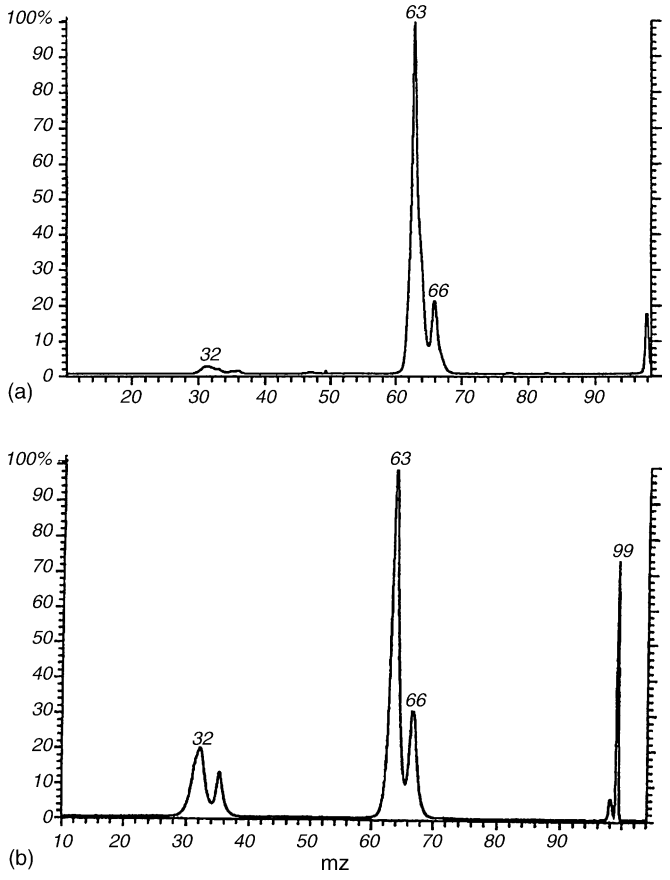


Fig. 5. (a) MIKES CID spectrum ($O_2$, 70% T) and (b) NR spectrum (Xe, 70% T/$O_2$, 70% T) of *m/z* 99 [P, $^{35}$Cl, S, H]$^+$ ions from ethylphosphonothioic dichloride (**III**).

All these structure indicative peaks indicates Cl–P–SH$^+$ (**2a**$^+$) bond connectivity for the *m/z* 99 ions.

### 3.6. Ion structures and energetics

From the computational results presented in Table 4, the potential energy diagram of Scheme 4, and the optimized ion structures shown in Fig. 6, it follows that all the four isomeric ions **2a**$^+$–**2d**$^+$ are minima on the potential energy surface. Ion **2a**$^+$ is the most stable structure of the four studied. It has a $C_S$ symmetry with anti arrangement of the S–H and Cl bonds that corresponds to the lowest-energy orientation of the corresponding bond dipoles. Ions **2b**$^+$ and **2c**$^+$ are 14.1 and 28.9 kcal mol$^{-1}$ less stable than **2a**$^+$ respectively. Ions **2a**$^+$ and **2b**$^+$ are separated by an energy barrier (35.5 kcal mol$^{-1}$ above **2b**$^+$). Similarly, **2b**$^+$

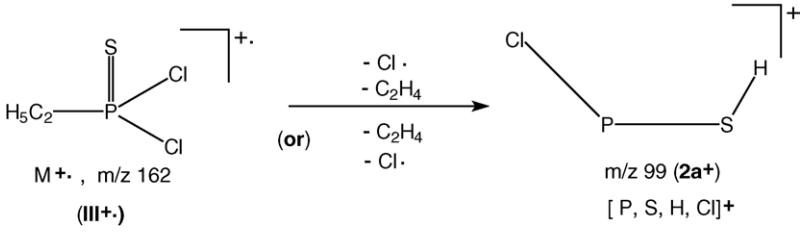


Scheme 3.

Table 4
Total (a.u.) and relative energies (kcal mol$^{-1}$) of [P, S, H, Cl]$^+$ ions calculated using various methods

| Species | G2 (0 K) | G2(MP2) (0 K) | B3LYP/6-31G(d, p)[a] |
|---|---|---|---|
| ClPSH$^+$ (**2a**$^+$) ($C_S$) | −1198.709273 (0.0) | −1198.694140 (0.0) | −1200.033640 (0.0) |
| HP(S)Cl$^+$ (**2b**$^+$) ($C_S$) | −1198.691582 (11.1) | −1198.676197 (11.3) | −1200.011118 (14.1) |
| HPSCl$^+$ (**2c**$^+$) ($C_S$) | −1198.664788 (27.9) | −1198.649999 (27.7) | −1199.987601 (28.9) |
| SP–ClH$^+$ (**2d**$^+$) ($C_S$) | −1198.697851 (7.2) | −1198.682900 (7.1) | −1200.0263859 (4.6) |
| TS **2a**$^+$–**2b**$^+$ ($C_S$) | −1198.630006 (49.7) | −1198.616223 (48.9) | −1199.954656 (49.6) |
| TS **2b**$^+$–**2c**$^+$ ($C_1$) | −1198.597440 (70.2) | −1198.581363 (70.8) | −1199.926387 (67.3) |
| TS **2a**$^+$–**2d**$^+$ ($C_S$) | −1198.656848 (32.9) | −1198.642807 (32.2) | −1199.978690 (34.5) |
| TS **2b**$^+$–**2d**$^+$ ($C_S$) | −1198.616395 (58.3) | −1198.602130 (57.7) | −1199.938918 (59.4) |
| PSH$^{\bullet+}$ + Cl$^\bullet$ $m/z$ 64 | −1198.566661 (89.5) | −1198.552653 (88.8) | −1199.916258 (73.6) |
| PS$^+$ + HCl $m/z$ 63 | −1198.686353 (14.4) | −1198.671173 (14.4) | −1200.010790 (14.3) |
| PCl$^{\bullet+}$ + SH$^\bullet$ $m/z$ 66 | −1198.56324 (91.6) | −1198.545953 (92.9) | −1199.902752 (82.1) |
| ClPS$^{\bullet+}$ + H$^\bullet$ $m/z$ 98 | −1198.569435 (87.7) | −1198.053601 (88.2) | −1199.898188 (84.9) |

[a] ZPE corrected.

and **2c**$^+$ ions are separated by an energy barrier (38.4 kcal mol$^{-1}$ above **2c**$^+$). Thus it is likely that most of the $m/z$ 99 ions will have Cl–P–SH$^+$ (**2a**$^+$) structure and significant contribution of **2b**$^+$–**2c**$^+$ can be ruled out.

The isomer **2d**$^+$ (dimer of PS and ClH) is second most stable isomer, 4.6 kcal mol$^{-1}$ less stable than **2a**$^+$. Ions **2a**$^+$ and **2d**$^+$ are separated by an energy barrier (29.9 kcal mol$^{-1}$ above **2d**$^+$), which is above the dissociation energy for the formation of PS$^+$ + HCl (14.3 kcal mol$^{-1}$). This implies that loss of HCl involves isomerization of **2a**$^+$ to **2d**$^+$ prior to dissociation. **2d**$^+$ is also separated from **2b**$^+$ by an energy barrier (45.3 kcal mol$^{-1}$ above **2b**$^+$). Thus based on all these results, it can be proposed that the CID spectra of $m/z$ 99 ions represent a mixture of **2a**$^+$/**2d**$^+$ ions. However, for energetic and entropic reasons most of the ions are expected to have the connectivity **2a**$^+$.

### 3.7. Preparation and dissociation of [P, Cl, S, H]$^\bullet$ radicals

The neutralization (Xe, 70%)–reionization ($O_2$, 70%) mass spectrum of $m/z$ 99 ions displays abundant recovery signal (75% of the base peak at $m/z$ 63) (Fig. 5b). The spectrum shows all the fragment ions that are seen in the CID spectrum of Fig. 5a, except that the relative abundances of $m/z$ 66, $m/z$ 32 and $m/z$ 35 are increased in the NR spectrum. The presence of an

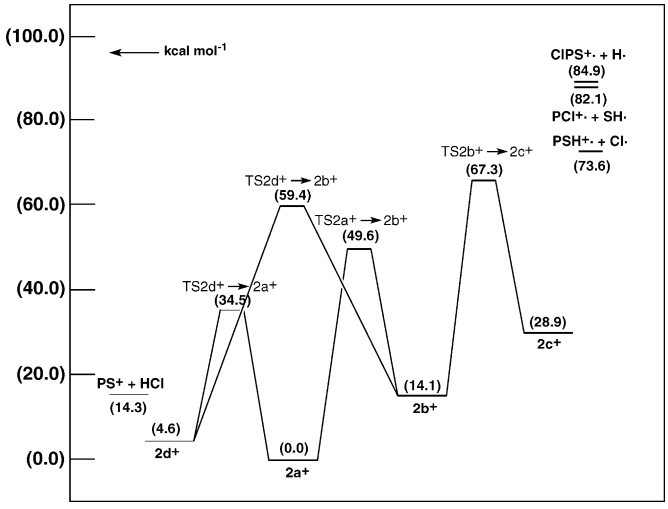


Scheme 4. Potential energy diagram from B3LYP/6-31G(d, p) calculations for the rearrangment and dissociation reactions of ions **2a**$^+$–**2d**$^+$.

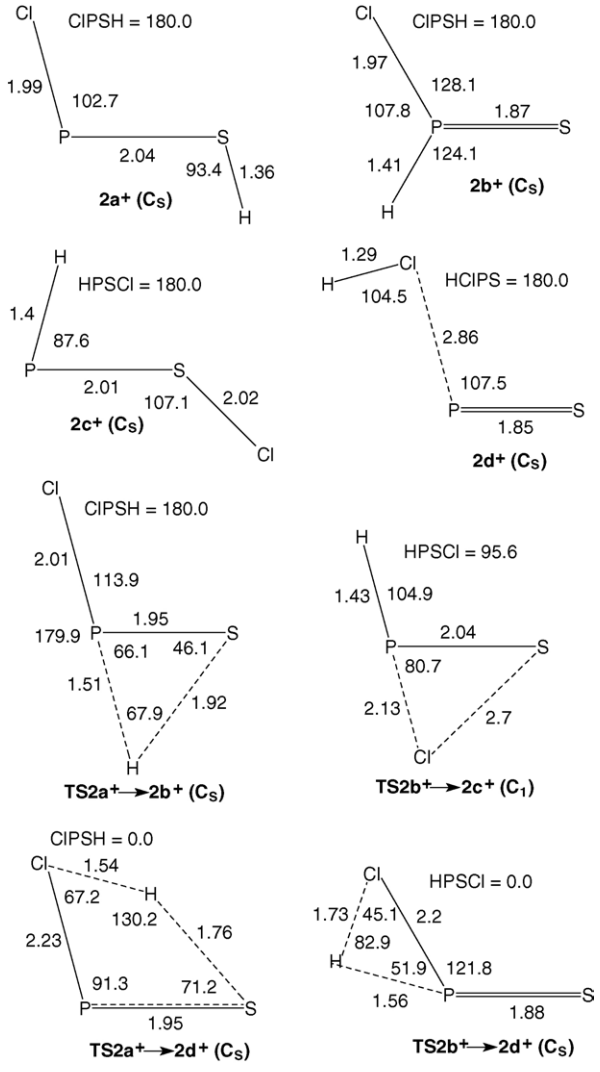


Fig. 6. Selected optimized geometries of ionic [P, Cl, S, H]$^+$ isomers **2a**$^+$–**2d**$^+$, connecting transition states from B3LYP/6-31G(d, p) calculations.

Table 5
Total (a.u.) and relative energies (kcal mol$^{-1}$) of [P, S, H, Cl] radicals calculated using various methods

| Species | G2 (0 K) | G2(MP2) (0 K) | B3LYP/6-31G(d, p)[a] |
|---|---|---|---|
| ClPSH$^{\bullet}$ (**2a**$^{\bullet}$) ($C_1$) | −1198.997643 (0.0) | −1198.979790 (0.0) | −1200.334619 (0.0) |
| HP(S)Cl$^{\bullet}$ (**2b**$^{\bullet}$) ($C_1$) | −1198.991950 (3.6) | −1198.974433 (3.4) | −1200.328883 (3.6) |
| HPSCl$^{\bullet}$ (**2c**$^{\bullet}$) ($C_1$) | −1198.959375 (24.0) | −1198.941471 (24.1) | −1200.306472 (17.7) |
| PS–HCl$^{\bullet}$ (**2d**$^{\bullet}$) ($C_S$) | | | −1200.311801 (14.3) |
| TS **2a**$^{\bullet}$–**2b**$^{\bullet}$ ($C_1$) | −1198.958425 (24.6) | −1198.940763 (24.5) | −1200.294311(25.3) |
| TS **2b**$^{\bullet}$–**2c**$^{\bullet}$ ($C_1$) | −1198.922048 (47.4) | −1198.903652 (47.8) | −1200.267908 (41.9) |
| ClPS + H$^{\bullet}$ *m*/*z* 99 | −1198.932011 (41.2) | −1198.915541 (40.3) | −1200.261195 (46.1) |
| PSH + Cl$^{\bullet}$ *m*/*z* 64 | −1198.872509 (78.5) | −1198.852092 (80.1) | −1200.2112643 (77.4) |
| Cl$^{\bullet}$ + PSH *m*/*z* 35 | −1198.872509 (78.5) | −1198.852092 (80.1) | −1200.2112643 (77.4) |
| PS$^{\bullet}$ + HCl *m*/*z* 63 | −1198.970953 (16.7) | −1198.95304 (16.8) | −1200.309704 (15.6) |
| PCl + SH$^{\bullet}$ *m*/*z* 66 | −1198.864228 (83.7) | −1198.843744 (85.4) | −1200.200834 (83.9) |

[a] ZPE corrected.

abundant recovery signal, indicates that vertical neutralization of **2a**$^{+}$ ions yield neutral species that are stable on the NR experimental time-scale of microseconds and have retained the **2a**$^{\bullet}$ connectivity. However, the vertical neutralization of other isomeric ions (**2b**$^{+}$–**2b**$^{+}$) that are co-generated with **2a**$^{+}$ in minor proportion seems to produce energized neutral species. These can undergo dissociation to generate various neutral/radical species such as PCl, S, Cl$^{\bullet}$, and PS$^{\bullet}$ which, on collisional reionization, may contribute to the enhancement of fragment ion abundances in the NR mass spectra.

### 3.8. Radical structures and energetics

These experimental results are consistent with the theoretical calculations (Table 5 and Fig. 7), which predict that **2a**$^{\bullet}$ is the global minimum and stable with respect to dissociation. In contrast to the cation relative stabilities, **2b**$^{\bullet}$ is second most stable isomer and 3.6 kcal mol$^{-1}$ less stable than **2a**$^{\bullet}$. **2a**$^{\bullet}$ and **2b**$^{\bullet}$ are separated by a substantial energy barrier of 25.3 kcal mol$^{-1}$. **2c**$^{\bullet}$ is 17.7 kcal mol$^{-1}$ less stable than **2a**$^{\bullet}$. Similarly to **1d**$^{\bullet}$, **2d**$^{\bullet}$ has optimized (B3LYP) to a structure different from **2d**$^{+}$, which is 14.3 kcal mol$^{-1}$ less stable than **2a**$^{\bullet}$. However, G2 calculations predict that **2d**$^{\bullet}$ is unstable towards dissociation and not a minima on the potential energy surface.

Further support for the stability of the transient neutral comes from an examination of the Franck–Condon effects on vertical electron capture by the corresponding cations. For **2a**$^{+}$, the calculated vertical ionization energy of the neutral ($IE_V$) is found to be 4.1 kcal mol$^{-1}$ (Table 6) higher than the adiabatic process, and vertical neutralization ($RE_V$) of thermalized Cl–P–SH$^{+}$ ions differ by only 5.8 kcal mol$^{-1}$ from the adiabatic process. The minimum excess Franck–Condon energy of Cl–P–SH$^{\bullet}$ is only 5.8 kcal mol$^{-1}$, which is insufficient to induce any dissociation or isomerization as the threshold energy of dissociation or isomerization lies at higher energies (Table 6). Thus the observed recovery signal in the NR spectrum should correspond to the **2a**$^{\bullet}$ survivor ions.

In contrast, vertical neutralization of **2d**$^{+}$ leads to **2d**$^{\bullet}$ with a different structure which probably dissociate into PS$^{\bullet}$ + HCl. Also neutralization of **2b**$^{+}$ and **2c**$^{+}$ can lead to **2b**$^{\bullet}$ and **2c**$^{\bullet}$ with internal energies (Table 6) that are sufficient to induce fragmentation. These neutral species, PS$^{\bullet}$ and other dissociation products P$^{\bullet}$, Cl$^{\bullet}$, on re-ionization can contribute to the enhancement of the signals at *m*/*z* 63, *m*/*z* 31 and *m*/*z* 35 in the NR spectrum. Thus it can be safely concluded that the neutral Chloro(thiohydroxy) phosphanyl ClPSH$^{\bullet}$ (**2a**$^{\bullet}$) is a viable species in the rarefied gas phase.

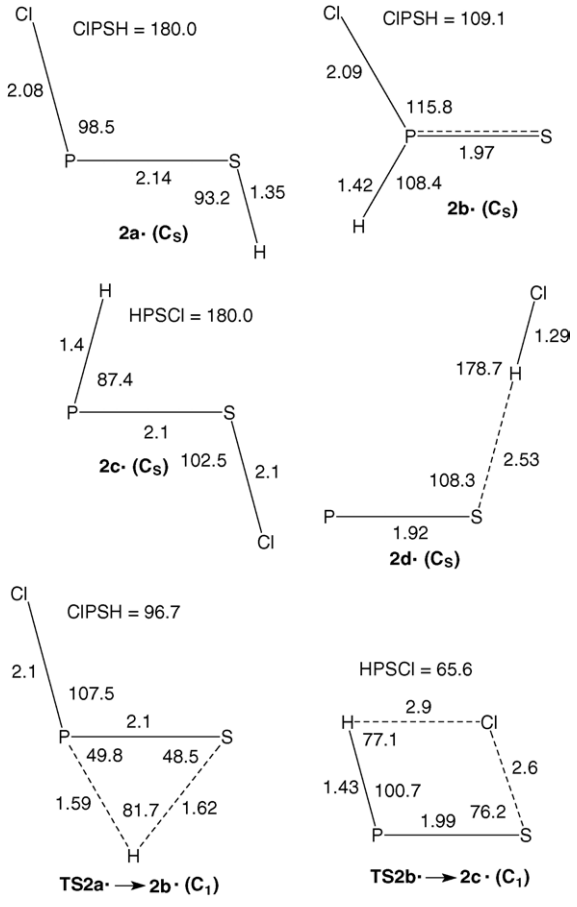


Fig. 7. Selected optimized geometries of neutral [P, Cl, S, H]$^{\bullet}$ isomers **2a**$^{\bullet}$–**2d**$^{\bullet}$ and connecting transition states from B3LYP/6-31G(d, p) level.

Table 6
Calculated adiabatic energies ($IE_a$) and vertical one-electron transition energies (in eV) of ions and neutrals of $[P, S, H, Cl]^{+/\bullet}$ isomers at B3LYP/6-31G(d, p) level

| Transitions | $IE_a$ | $RE_v$ | $IE_v$ |
|---|---|---|---|
| $\mathbf{2a}^+ \rightarrow \mathbf{2a}^\bullet$ | 8.16 | 7.91 | |
| $\mathbf{2a}^\bullet \rightarrow \mathbf{2a}^+$ | | | 8.34 |
| $\mathbf{2b}^+ \rightarrow \mathbf{2b}^\bullet$ | 8.62 | 7.77 | |
| $\mathbf{2b}^\bullet \rightarrow \mathbf{2b}^+$ | | | 9.57 |
| $\mathbf{2c}^+ \rightarrow \mathbf{2c}^\bullet$ | 8.36 | 8.14 | |
| $\mathbf{2c}^\bullet \rightarrow \mathbf{2c}^+$ | | | 8.50 |

$RE_v$ and $IE_v$ represents recombination (neutralization) and ionization energies, respectively.

## 4. Conclusions

From the combined results of mass spectrometric experiments and theoretical calculations at B3LYP/6-31G(d, p) and G2/G2(MP2) levels, it is proposed that dissociative electron ionization of diethyl chlorothiophosphate (**I**) and ethylphosphonodichloridate (**II**) yields bi co-ordinateed chloro(hydroxy) phosphanyl $[Cl–P–OH]^+$ ions and ethylphosphonothioic dichloride (**III**) affords chloro(thiohydroxy) phosphanyl $[Cl–P–SH]^+$ ions. Collision induced dissociation mass spectra of $[Cl–P–OH]^+$ and $[Cl–P–SH]^+$ ions are used to deduce their connectivities. NR experiments confirmed the theoretical prediction that neutral $[Cl–P–OH]^\bullet$ and $[Cl–P–SH]^\bullet$ are a stable species in the rarefied gas phase.

## Acknowledgements

The authors thank Dr. J.S. Yadav, Director, IICT, Hyderabad, for facilities and Dr. M. Vairamani and Dr. B.M. Choudary for cooperation. R.S.K and P.N.R thanks CSIR, New Delhi, for the awards of Senior Research Fellowship.

## References

[1] A.H. Cowley, Acc. Chem. Res. 17 (1984) 386.
[2] A.H. Cowley, Polyhedron 3 (1984) 389.
[3] W.W. Schoeller, in: M. Regitz, O. Scherer (Eds.), Multiple Bonds and Low Coordination in Phosphorus Chemistry, Georg Thieme-Verlag, Stuttgart, 1990, p. 5.
[4] O.J. Scherer, Angew. Chem. Int. Ed. Engl. 97 (1985) 924.
[5] M. Sanchez, M.R. Mazieres, L. Lamande, R. Wolf, in: M. Regitz, O. Scherer (Eds.), Multiple Bonds and Low Coordination in Phosphorus Chemistry, Georg Thieme-Verlag, Stuttgart, 1990, p. 129.
[6] G.J. Kruger, S. Lotz, L. Linford, M. Vandtk, H.G. Raubenheimer, J. Organomet. Chem. 280 (1985) 241.
[7] E. Lindner, K. Auch, G.A. Weiss, W. Hiller, R. Fawzi, Chem. Ber. 119 (1986) 3076.
[8] C. Wesdemiotis, F.W. McLafferty, Chem. Rev. 87 (1987) 485.
[9] J.L. Holmes, Mass Spectrom. Rev. 8 (1989) 513.
[10] F. Tureček, Org. Mass Spectrom. 27 (1992) 1087.
[11] D.V. Zagorevski, J.L. Holmes, Mass Spectrom. Rev. 13 (1994) 133.
[12] N. Goldberg, H. Schwarz, Acc. Chem. Res. 27 (1994) 347.
[13] D.V. Zagorevski, J.L. Holmes, Mass Spectrom. Rev. 18 (1999) 87.
[14] F. Tureček, Top. Curr. Chem. 225 (2003) 77.
[15] H. Keck, W. Kuchen, H. Renneberg, J.K. Terlouw, H.C. Visser, Angew. Chem. Int. Ed. Engl. 30 (1991) 318.
[16] H. Keck, W. Kuchen, H. Renneberg, J.K. Terlouw, Phosphorus Sulfur Rel. Elem. 40 (1988) 227.
[17] H. Keck, W. Kuchen, H. Renneberg, J.K. Terlouw, H.C. Visser, Z. Anorg. Allg. Chem. 580 (1990) 181.
[18] T. Wong, J.K. Terlouw, H. Keck, W. Kuchen, P. Tommes, J. Am. Chem. Soc. 114 (1992) 8208.
[19] H. Keck, W. Kuchen, H. Renneberg, A. Schweighofer, J.K. Terlouw, Phosphorous Sulphur Silicon 104 (1995) 189.
[20] M. Gu, F. Tureček, Org. Mass Spectrom. 28 (1993) 1135.
[21] S. Vivekananda, R. Srinivas, Int. J. Mass Spectrom. Ion Process. 171 (1997) 79.
[22] S. Vivekananda, P. Raghunath, K. Bhanuprakash, R. Srinivas, Int. J. Mass Spectrom. 208 (2001) 59.
[23] L.N. Heydorn, C.Y. Wong, R. Srinivas, J.K. Terlouw, Int. J. Mass Spectrom. 225 (2003) 11.
[24] F. Tureček, M. Gu, C.E.C.A. Hop, J. Phys. Chem. 99 (1995) 2278.
[25] S.M. Gustafson, C.J. Cramer, J. Phys. Chem. 99 (1995) 2267.
[26] C.J. Cramer, S.M. Gustafson, J. Am. Chem. Soc. 116 (1994) 723.
[27] C.J. Cramer, S.M. Gustafson, J. Am. Chem. Soc. 115 (1993) 9315.
[28] C.J. Cramer, Chem. Phys. Lett. 202 (1993) 297.
[29] C.J. Cramer, J. Am. Chem. Soc. 113 (1991) 2439.
[30] C.J. Cramer, J. Am. Chem. Soc. 112 (1990) 7965.
[31] C.J. Cramer, C.E. Dykstra, S.E. Denmark, Chem. Phys. Lett. 136 (1987) 17.
[32] M. Korn, H. Oberhammer, R. Minkwitz, J. Mol. Struct. 300 (1993) 61.
[33] R. Srikanth, R. Srinivas, K. Bhanuprakash, S. Vivekananda, E.A. Syrstad, F. Tureček, J. Am. Soc. Mass Spectrom. 13 (2002) 250.
[34] R. Srikanth, P. Nagi Reddy, K. Bhanuprakash, R. Srinivas, X. Chen, F. Tureček, J. Am. Soc. Mass Spectrom. 16 (2005) 1353.
[35] J.P. Clay, J. Org. Chem. 16 (1951) 892.
[36] F.W. Hoffmann, D.H. Wadsworth, H.D. Weiss, J. Am. Chem. Soc. 80 (1958) 3945.
[37] M.J. Frisch, G.W. Trucks, H.B. Schlegel, G.E. Scuseria, M.A. Robb, J.R. Cheeseman, J.A. Montgomery, T. Vreven, K.N. Kudin, J.C. Burant, J.M. Millam, S.S. Iyengar, J. Tomasi, V. Barone, B. Mennucci, M. Cossi, G. Scalmani, N. Rega, G.A. Petersson, H. Nakatsuji, M. Hada, M. Ehara, K. Toyota, R. Fukuda, J. Hasegawa, M. Ishida, T. Nakajima, Y. Honda, O. Kitao, H. Nakai, M. Klene, X. Li, J.E. Knox, H.P. Hratchian, J.B. Cross, C. Adamo, J. Jaramillo, R. Gomperts, R.E. Stratmann, O. Yazyev, A.J. Austn, R. Cammi, C. Pomelli, J.W. Ochterski, P.Y. Ayala, K. Morokuma, G.A. Voth, P. Salvador, J.J. Dannenberg, V.G. Zakrzewski, S. Dapprich, A.D. Daniels, M.C. Strain, O. Farkas, D.K. Malick, A.D. Rabuck, K. Raghavachari, J.B. Foresman, J.V. Ortiz, Q. Cui, A.G. Baboul, S. Clifford, J. Cioslowski, B.B. Stefanov, G. Liu, A. Liashenko, P. Piskorz, I. Komaromi, R.L. Martin, D.J. Fox, T. Keith, M.A. Al-Laham, C.Y. Peng, A. Nanayakkara, M. Challacombe, P.M.W. Gill, B. Johnson, W. Chen, M.W. Wong, C. Gonzalez, J.A. Pople, Gaussian 03, Revision B.05, Gaussian Inc., Pittsburgh PA, 2003.
[38] A.D. Becke, J. Chem. Phys. 98 (1993) 5648.
[39] L.A. Curtiss, K. Raghavachari, G.W. Trucks, J.A. Pople, J. Chem. Phys. 94 (1991) 7221.
[40] L.A. Curtiss, K. Raghavachari, G.W. Trucks, J.A. Pople, J. Chem. Phys. 98 (1993) 1293.
[41] F.A. Wiedman, J. Cai, C. Wesdemiotis, Rapid Commun. Mass Spectrom. 8 (1994) 804.